Supporting information for

Facile and processable integration strategy towards Schiff-base polymer derived carbonaceous materials with high lithium storage performance

Zhichang Xiao[a,c], Junwei Han[b], Jing Xiao[b], Qi Song[a], Xinghao Zhang[a,c], Debin Kong[a,b], Quan-Hong Yang[b], Linjie Zhi[a,b,c]**

a. CAS Key Laboratory of Nanosystem and Hierarchical Fabrication, CAS Center for Excellence in Nanoscience, National Center for Nanoscience and Technology, Beijing 100190, P. R. China
b. School of Chemical Technology and Engineering, Tianjin University, Tianjin 300350, P. R. China.
c. University of Chinese Academy of Sciences, Beijing 100049, P. R. China

Email: zhilj@nanoctr.cn; kongdb@nanoctr.cn

Contents:

Experimental Section

Synthesis of graphene foam (Gf) : Graphene oxide (GO) was synthesized from natural graphite (99.999%, 200 mesh) by a modified Hummers method. 20 mL deionized water was added into 20 mL GO solution (10 mg mL^{-1}), which were then added into Teflonlined autoclave. The solution was sealed and heated at 180 °C for 12 h and naturally cooled down to room temperature. The cylindrical GO hydrogel was immersed into liquid nitrogen for several minutes until the solution was fully solidified and then freeze-dried for 24 h. After freeze-dried, the GO foam was heated at 900 °C for 2 h under H_2 atmosphere to obtain the graphene foam (Gf).

Synthesis of graphene powder (Gp) : the procedure for synthesis of Gp was similar to that of Gf, except the GO foam was grinded into powder before the thermal reduction.

Synthesis of SNW/ Gf precursor and NEC/ Gf: melamine (0.4 mmol, 504.48 mg), and 1, 4-phthalaldehyde (0.3 mmol, 402.39 mg) were dissolved in DMSO (10 ml). After being stirred for 20 h at 80 ℃, the concentrated solution containing the Schiff-base oligomer was obtained. 1 mL concentrated solution was immersed into 20 mg Gf to get SNW/ Gf precursor, which was heated up to 500 ℃ with a heating rate of 5 ℃ min^{-1} under argon for 6 h to get the NEC/ Gf composite.

Synthesis of SNW/ Gp and NEC/ Gp: melamine (0.4 mmol, 504.48 mg), 1, 4-phthalaldehyde (0.3 mmol, 402.39 mg) and 50 mg Gp were dissolved in DMSO (5 ml). After being stirred for 72h at 180 ℃ under reflux, a gray solid powder (SNW/ Gp)

was obtained, which was heated up to 500 ℃ with a heating rate of 5 ℃ min^{-1} under argon for 6 h to get the NEC/ Gp composite.

Characterization: The structure is characterized by, X-ray diffraction (Rigaku D/max-2500B2+/PCX system), Fourier transform infrared spectrometer (FT-IR, Perkin, Spectrum One) and Raman spectra (Renishaw, Renishaw invia plus). The morphology is observed with field-emission transmission electron microscopy (FE-TEM) and scanning electron microscopy (SEM, Hitachi S4800). Scanning transmission electron microscopy (STEM) and elemental mapping images are collected from a Tecnai G2 F20 U-TWIN microscope with STEM-HAADF attachment. Nitrogen sorption isotherms are determined by nitrogen physisorption at 77 K on a Micrometritics ASAP 2020 analyzer. The pore size distribution (PSD) is calculated via a non-local density functional theory (NLDFT) method. X-ray photoelectron spectroscopy (XPS) measurement is conducted on an ESCALAB250Xi system with a monochromatic Al Kα X-ray source.

Electrochemical Measurements: The electrochemical performance of the NEC/ Gf is measured with the type of 2032 coin cells. Li metal is used as the counter electrode; 1 M $LiPF_6$ in ethylene carbonate (EC)/dimethyl carbonate (DMC) (1:1 by volume) is used as electrolyte, and Celgard 2300 as separator. The working electrodes are prepared by mixing the samples NEC/Gf or NEC/Gp, carbon black (Super-P), and poly(vinyl difluoride) (PVDF) at a weight ratio of 80:10:10 and pasting onto a copper foil substrate and then dried in a vacuum oven at 80 °C for 24 h. The cells are assembled in an argon-filled glove box with the concentrations of moisture and

oxygen below 1 ppm. The galvanostatic charge/discharge tests are carried out between 0.01-3.00 V vs. Li^+/Li on a Land CT2001A (China). Electrochemical impedance spectral measurements are carried out in the frequency in the range between 100 kHz and 10 mHz on a Biologic VSP electrochemical workstation.

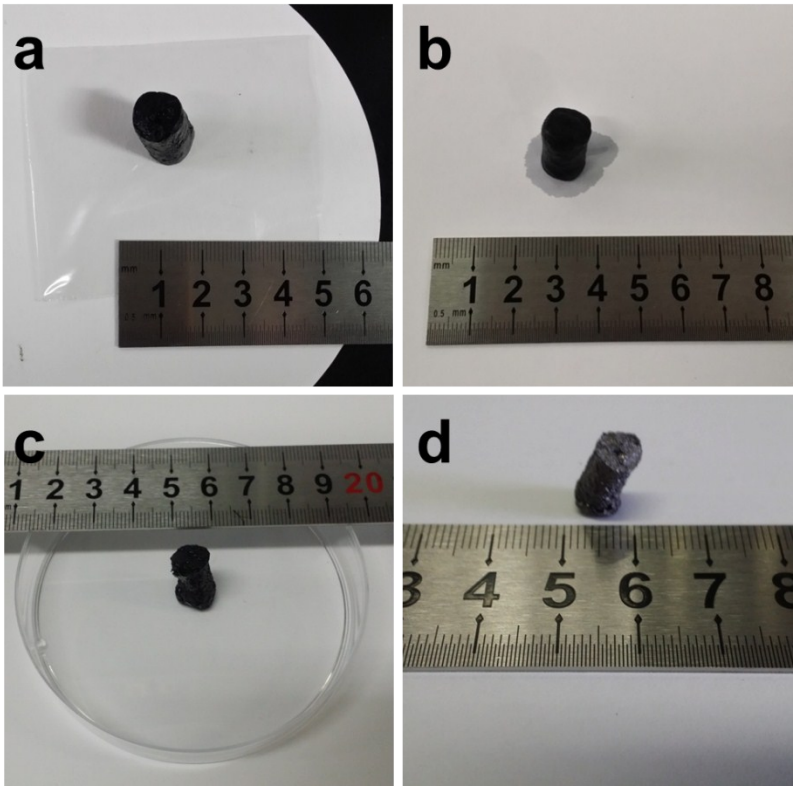

Fig. S1 Photographs to explain the integrity of SNW/ Gf during different steps. (a) GO hydrogel; (b) GO foam after adsorption of SNW concentrated solution; (c) SNW/ Gf after drying process; (d) SNW/ Gf after heat treatment.

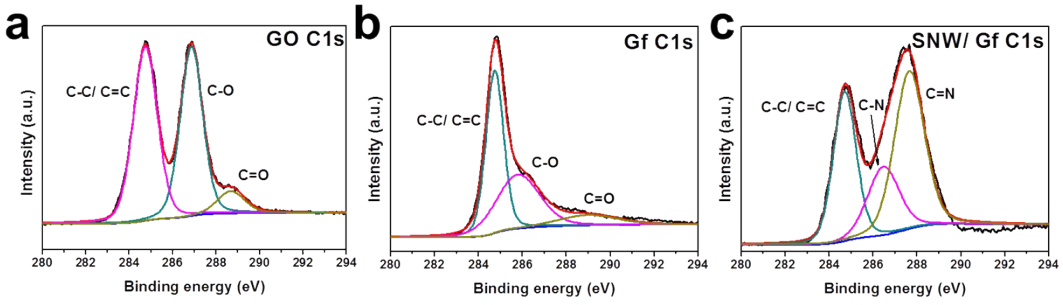

Fig. S2 C1s spectra of (a) GO; (b) Gf and (c) SNW/ Gf.

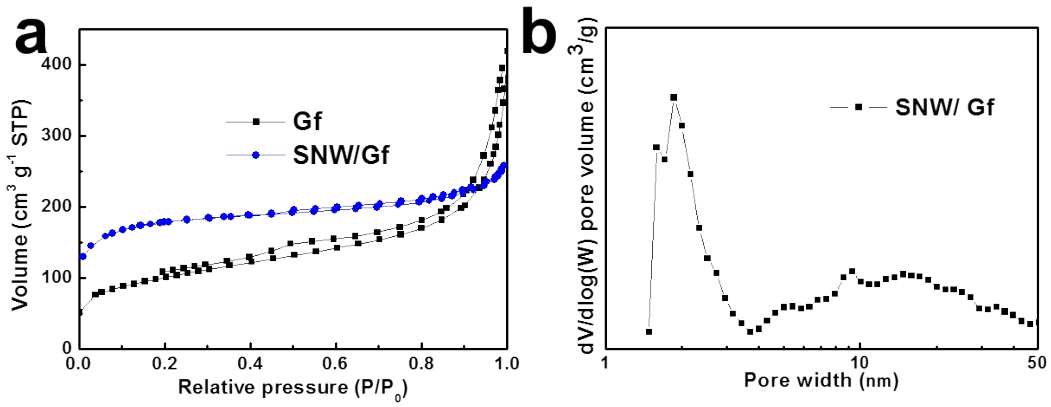

Fig. S3 (a) Nitrogen adsorption/ desorption isotherms of Gf and SNW/ Gf; (b) pore-size distribution of SNW/ Gf.

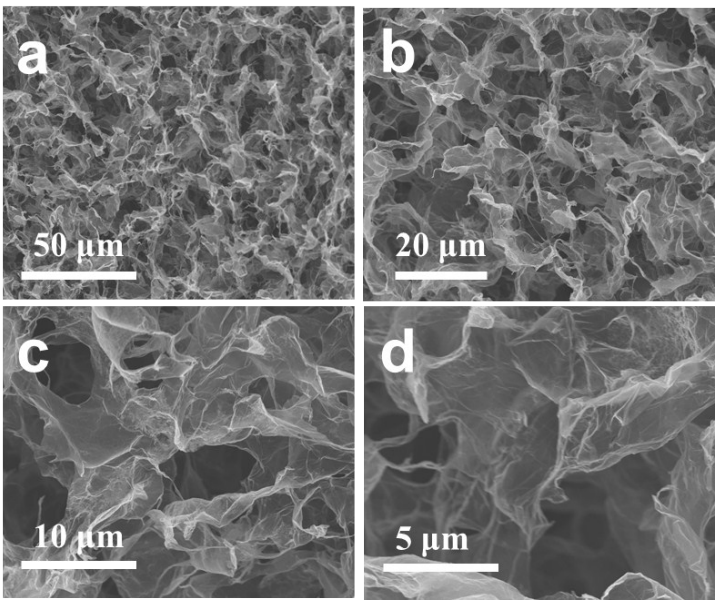

Fig. S4 SEM images of Gf at different magnifications.

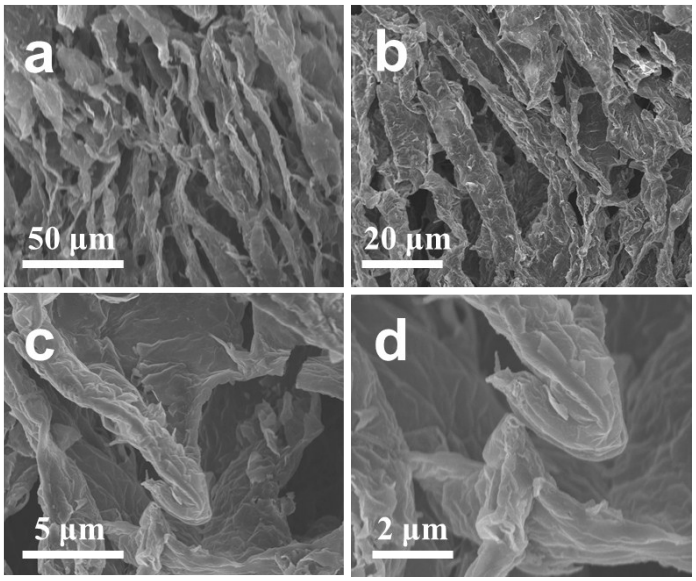

Fig. S5 SEM images of SNW/ Gf at different magnifications.

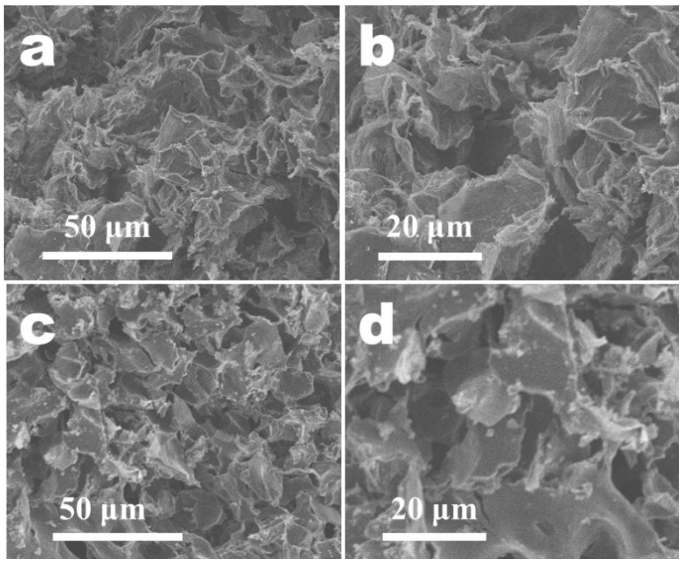

Fig. S6 SEM images of NEC/ Gp at different magnifications.

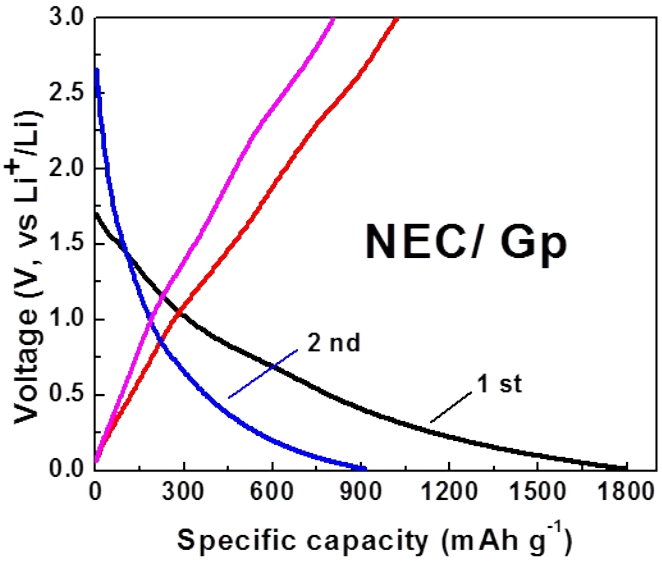

Fig. S7 Charge/ discharge curves of NEC/ Gp at a current density of 0.1 A g^{-1} between 0.01 and 3.0 V.

Table S1 Ratios of different nitrogen types for sample SNW/ Gf and NEC/ Gf

	SNW/ Gf	**NEC/ Gf**
Pyridinic N	48.7%	23%
Pyrrolic N	51.3%	50.8%
Quaternary N	--	25.6%

Table S2 Comparison of volumetric capacity between NEC/Gf and other related anodes.

sample	Volumetric capacity (mAh cm^{-3})	Current density	cycles	Ref
NEC/Gf	1000	0.1 A g^{-1}	500	This work
Commercial graphite	600	--	--	1
N-aC_{60}	117.4	100 mA g^{-1}	80	2
NEC/CNT-450	787.5	0.5 A g^{-1}	1000	3
NHGM	1052	0.1 mA cm^{-2}	1200	4
Si-C granule	779	2.98 A g^{-1}	100	5
SiNP-PANI	1078	1 A g^{-1}	>600	6

Table S3 Initial columbic efficiency of NEC/Gf and other carbonaceous materials as anodes in LIB.

Sample	intial columbic efficiency (%)	Ref
NEC/Gf	45	This work
Porous N/B-doped Graphene sheets	43.5	7
Porous carbon	48.3	8
Porous carbon nanofibers	42.5	9
Hollow carbon spheres	41.9	10
Porous carbon	38.8	11
Porous hard carbons	47.3	12
Macroporous carbon	42.9	13
Hollow carbon nanospheres	43.9	14

References

1. N. Liu, Z. Lu, J. Zhao, M. T. Mcdowell, H. W. Lee, W. Zhao and Y. Cui, *Nat. Nanotechnol.*, 2014, **9**, 187-192.

2. Z. Tan, K. Ni, G. Chen, W. Zeng, Z. Tao, M. Ikram, Q. Zhang, H. Wang, L. Sun, X. Zhu, X. Wu, H. Ji, R. S. Ruoff and Y. Zhu, *Adv. Mater.*, 2017, **29**, 1603414.
3. Z. Xiao, Q. Song, R. Guo, D. Kong, S. Zhou, X. Huang, R. Iqbal and L. Zhi, *Small*, 2018, **14**, 1703569.
4. X. Wang, L. Lv, Z. Cheng, J. Gao, L. Dong, C. Hu and L. Qu, *Adv. Energy Mater.*, 2016, **6**, 1502100.
5. A. Magasinski, P. Dixon, B. Hertzberg, A. Kvit, J. Ayala and G. Yushin, *Nat. Mater.*, 2010, **9**, 353-358.
6. H. Wu, G. Yu, L. Pan, N. Liu, M. T. Mcdowell, Z. Bao and Y. Cui, *Nat. Commun.*, 2013, **4**, 1943.
7. Z. S. Wu, W. Ren, L. Xu, F. Li and H. M. Cheng, *ACS Nano*, 2011, **5**, 5463-5471.
8. F. Zhang, K. X. Wang, G. D. Li and J. S. Chen, *Electrochem. Commun.*, 2009, **11**, 130-133.
9. Z. J. Fan, J. Yan, T. Wei, G. Q. Ning, L. J. Zhi, J. C. Liu, D. X. Cao, G. L. Wang and F. Wei, *ACS Nano*, 2011, **5**, 2787-2794.
10. S. Yang, X. Feng, L. Zhi, Q. Cao, J. Maier and K. Müllen, *Adv. Mater.*, 2010, **22**, 838-842.
11. J. Yi, X. P. Li, S. J. Hu, W. S. Li, L. Zhou, M. Q. Xu, J. F. Lei and L. S. Hao, *J.Power Sources*, 2011, **196**, 6670-6675.
12. J. Yang, X. Y. Zhou, J. Li, Y. L. Zou and J. J. Tang, *Mater. Chem. Phys.*, 2012, **135**, 445-450.
13. K. T. Lee, J. C. Lytle, N. S. Ergang, S. M. Oh and A. Stein, *Adv. Funct. Mater.*, 2010, **15**, 547-556.
14. F. D. Han, Y. J. Bai, R. Liu, B. Yao, Y. X. Qi, N. Lun and J. X. Zhang, *Adv. Energy Mater.*, 2011, **1**, 798-801.